

Reversible Concerted Metallation-Deprotonation C–H Bond Activation by [Cp*RhCl]

Andrew I VanderWeide, William W. Brennessel, and William D. Jones

J. Org. Chem., **Just Accepted Manuscript** • DOI: 10.1021/acs.joc.9b01716 • Publication Date (Web): 10 Sep 2019

Downloaded from pubs.acs.org on September 12, 2019

Just Accepted

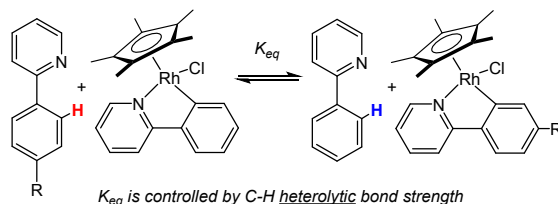
“Just Accepted” manuscripts have been peer-reviewed and accepted for publication. They are posted online prior to technical editing, formatting for publication and author proofing. The American Chemical Society provides “Just Accepted” as a service to the research community to expedite the dissemination of scientific material as soon as possible after acceptance. “Just Accepted” manuscripts appear in full in PDF format accompanied by an HTML abstract. “Just Accepted” manuscripts have been fully peer reviewed, but should not be considered the official version of record. They are citable by the Digital Object Identifier (DOI®). “Just Accepted” is an optional service offered to authors. Therefore, the “Just Accepted” Web site may not include all articles that will be published in the journal. After a manuscript is technically edited and formatted, it will be removed from the “Just Accepted” Web site and published as an ASAP article. Note that technical editing may introduce minor changes to the manuscript text and/or graphics which could affect content, and all legal disclaimers and ethical guidelines that apply to the journal pertain. ACS cannot be held responsible for errors or consequences arising from the use of information contained in these “Just Accepted” manuscripts.

Reversible Concerted Metallation-Deprotonation C–H Bond Activation by $[\text{Cp}^*\text{RhCl}_2]_2$

Andrew I. VanderWeide, William W. Brennessel, William D. Jones*

Department of Chemistry, University of Rochester, Rochester, NY 14627

Email: jones@chem.rochester.edu



ABSTRACT: The reversibility of the concerted metallation-deprotonation exchange of eight para-substituted phenylpyridines is examined with the parent $\text{Cp}^*\text{RhCl}(\kappa\text{-C}, N\text{-NC}_5\text{H}_4\text{-C}_6\text{H}_4)$. Equilibrium constants are determined, and the free energies are used to extract the most important parameters that control the thermodynamics. K_{eq} values are found to correlate best with heterolytic C–H bond strengths, but in a way that is not obvious considering the electrophilic nature of these activations.

INTRODUCTION

The electrophilic activation and functionalization of aromatic C–H bonds is rapidly being recognized as one of the most important transformations in organic methodology.¹ Heck showed as early as 1975 that palladium(II) metallacycles formed via directed cyclometallation could be carbonylated to give heterocycles.² Pfeffer also reported a number of examples in which metallacycles of palladium(II) and ruthenium(II) reacted with alkynes to give heterocycles.^{3,4} Our group demonstrated the use of alkynes for conversion of metallacycles to isoquinolines with $[\text{Cp}^*\text{RhCl}_2]_2$.⁵ Importantly, Fagnou first showed that catalytic $[\text{Cp}^*\text{RhCl}_2]_2$ could be used with $\text{Cu}(\text{OAc})_2$ for the synthesis of indoles⁶ and isoquinolines.⁷

In the 1980's, Ryabov used kinetics to examine the mechanism of cyclometallation of dimethylbenzylamine by palladium acetate and concluded that a coordinated acetate deprotonated a ligated amine while forming the Pd–aryl bond.⁸ A Hammett rho value of +1.4 was seen for the rate of activation, as electron-withdrawing substituents resulted in a higher rate of reaction. This result is similar to the related directed functionalizations using lower oxidation state metals that operate via C–H oxidative addition.⁹ The electrophilic cleavage of the aromatic C–H bond adjacent to a coordinating functional group using acetate as base and Ru, Rh, and Ir was studied extensively by Davies,^{10–13} and has come to be referred to as ‘concerted metallation-deprotonation’, or CMD.¹⁴

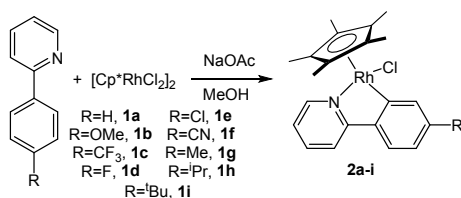
Our group has examined the kinetics of concerted metallation-deprotonation of arylimines with electron-donating and –withdrawing groups at Cp^*Rh and Cp^*Ir centers, and found that C–H activation proceeds by a $[\text{Cp}^*\text{M}(\text{OAc})\text{L}]^+$ fragment.¹⁵ It was found that the C–H activation was reversible, slowly, with acetic acid but was much more rapid if trifluoroacetic acid was added. This observation is consistent with ortho-deuteration of unreacted substrate seen in catalytic

work by Fagnou with $[\text{Cp}^*\text{RhCl}_2]_2$.⁶ Examination of 11 different carboxylates showed that with some, cyclometallation of 4-(2-pyridinyl)anisole went to equilibrium, not completion.¹⁶ In this report, we examine the reversibility of the concerted metallation-deprotonation of a variety of para-substituted phenylpyridines, and use equilibration data to examine the factors that control the thermodynamics of the C–H activation.

RESULTS AND DISCUSSION

Metallacycle Synthesis. Syntheses of the C–H activated complexes shown in Scheme 1 were adapted from known procedures.¹⁵ These reactions are believed to follow the CMD pathway, where in the presence of NaOAc, $[\text{Cp}^*\text{RhCl}_2]_2$ generates a $[\text{Cp}^*\text{Rh}(\kappa^2\text{-OAc})\text{L}]^+$ species. Coordination of 2-phenylpyridine leads to C–H activation via deprotonation by the acetate ligand as the aryl group bonds to the rhodium.¹² Each of the C–H activated complexes were generated by reaction of $[\text{Cp}^*\text{RhCl}_2]_2$ with the substituted 2-phenylpyridines, **1a–i**, in the presence of sodium acetate (Scheme 1). All products were thoroughly characterized by NMR spectroscopy, elemental analysis, and single-crystal structural determination. For **2c**, **2e**, and **2g–i** X-ray quality crystals were obtained by cooling a saturated solution in methanol. For **2f**, X-ray quality crystals were obtained by diffusion of pentane into benzene. The remaining complexes (**2a**, **2b**, **2d**) have previously published crystal structures.¹⁷ Structural parameters will be commented on in conjunction with equilibration data (*vide infra*).

Scheme 1.



Equilibration Experiments. As earlier studies indicated that C–H activation by the CMD process is reversible, equilibrium constants for exchange of one substrate for another should be measurable (eq 1). In Figure 1, the iminyl region of the ^1H NMR spectrum is shown for the equilibration of parent complex **2a** and 4-(2-pyridinyl)anisole **1b**. Here, **2a** was prepared in situ using $[\text{Cp}^*\text{RhCl}_2]_2$ and 1 equiv phenylpyridine in the presence of a 5-fold excess of sodium acetate. Once formation of **2a** was complete, 1 equiv of **1b** was added. The iminyl signals are distinct for all 4 species involved in this equilibrium and appear as doublets. The iminyl signal for **2a** appears at δ 8.77 and the corresponding signal for unactivated substrate **1b** appears at δ 8.51. Similarly, **2b** has an iminyl doublet at δ 8.69, and the unactivated substrate **1a** appears at δ 8.57.

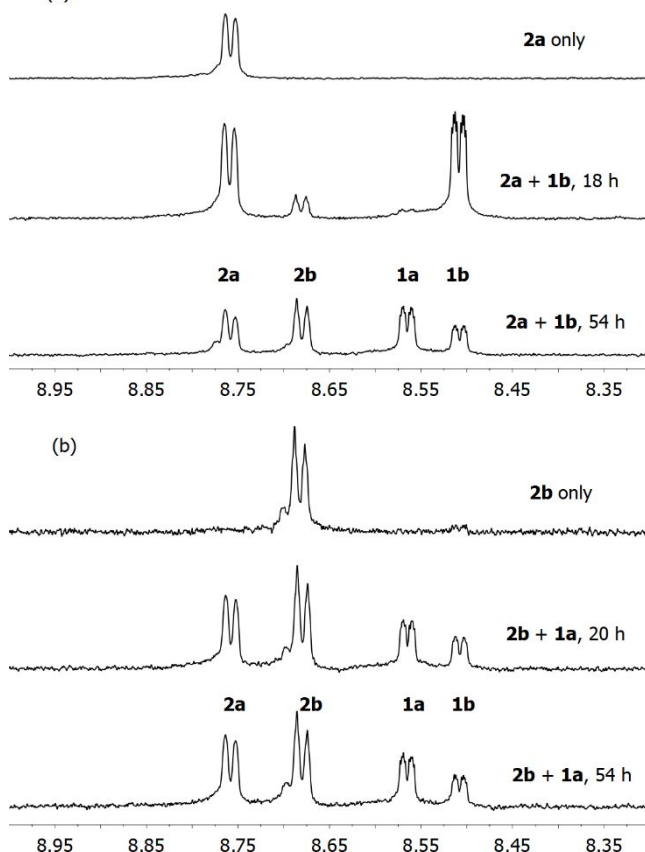
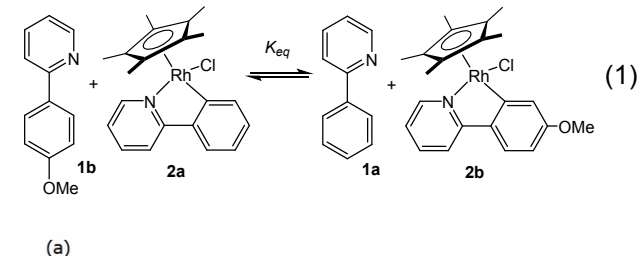


Figure 1. Equilibration of **2a** + **1b** with **2b** + **1a** (a) approaching from the left and (b) approaching from the right.

When C–H activated complex **2a** is exposed to 4-(2-pyridinyl)anisole, **1b**, two new peaks slowly appear: one corresponding to phenylpyridine substrate **1a**, and one corresponding to the C–H activated complex **2b** generated via exchange. Over the next few days the reaction was heated to 40 °C and the equilibrium constant was calculated from the integrations of these resonances (Figures 1a and S10 to S17). To ensure this exchange had reached equilibrium, a similar experiment was performed starting from the opposite side of the equilibrium, in this case combining C–H activated complex **2b** with phenylpyridine **1a** (Figure 1b). In this way the equilibrium was approached from both the left and the right, and the reaction is guaranteed to be at equilibrium if the same K_{eq} is observed.

In many cases, for inconsistent and unknown reasons, equilibration from both directions did not reach the same equilibrium position. Moreover, in the rare cases that these reactions did reach the same point of equilibration they took weeks to months to reach equilibrium. The 5-fold excess of NaOAc used to prepare **2a** drives the C–H activation to completion and produces only a small amount of acetic acid in the process. It was hypothesized that the long equilibration time was because this small amount of acetic acid produced is not sufficient to catalyze the reverse C–H activation to completion. Therefore, a 5-fold excess of acetic acid was added to the reaction following the formation of **2a**. This 1:1 sodium acetate : acetic acid buffer allows for both the forward and reverse reactions to go to completion more rapidly, typically 40-50 hrs. While the mechanism of the exchange was not examined in detail, the above observation is consistent with a pathway involving the microscopic reverse of the way these compounds were formed: exchange of chloride for acetic acid followed by protonation of the Rh-aryl bond to liberate phenylpyridine and product $[\text{Cp}^*\text{Rh}(\text{OAc})]^+$, which then activates the added substituted phenylpyridine via CMD. Under reaction conditions (acetate buffer in methanol solvent), only the starting materials and products are observed – the pyridines **1a-i** are not protonated, nor are the chloride ligands replaced in compounds **2** (See Supporting Information, Fig. S27).

Similar experiments were performed with the remaining substrates. In some cases the iminyl NMR resonances of a substrate or metallacycle overlap with one another. In these cases, the equilibrium was measured relative to another substrate where there was no overlap of the iminyl resonances, and then this K_{eq} was referred back to the parent phenylpyridine K_{eq} . These equilibrium constants are listed in Table 1. As can be seen, the K_{eq} values vary only slightly, with substrates with electron-withdrawing groups being favored.

Equilibration experiments were attempted with additional electron-rich substrates, however amines were not chemically compatible with this equilibration experiment. For the corresponding dimethylamino substrate, with the 1:1 sodium acetate acetic acid buffer, both protonated and deprotonated amines in both the substrate and the C–H activated complex were observed to equilibrate. Due to the complexity of these equilibria, it was not possible to collect meaningful K_{eq} data.

The ΔG values for these equilibria with **2a** can be obtained from the K_{eq} values, and are also listed in Table 1. It was found that there is a reasonably good correlation of $\log K_{\text{eq}}$ with the Hammett σ_m -value for the para substituent on the phenylpyridine (Fig. 2). The correlation with σ_m indicates that the electron-donating/withdrawing power of the substituent is responsible for affecting the equilibrium. The ρ value of +1.34 (20) indicates that electron withdrawing groups favor a shift of

the equilibrium toward activation of that phenylpyridine substrate.

Table 1. Measured K_{eq} of 4-R-(2-pyridyl)arene substrates relative to 2-phenylpyridine in methanol at 40 °C in the presence of 0.05 M NaOAc/HOAc buffer (eq 1).^a

Substrate	K_{eq}	ΔG^0 kcal/mol	$d_{Rh-aryl}$ Å	d_{Rh-N} Å
R = H, 1a ^b	1.0	0.0	2.0361 (13)	2.0917 (12)
R = OMe, 1b ^c	2.0 (8)	-0.44 (25)	2.0209 (15)	2.1000 (15)
R = CF ₃ , 1c	6.3 (25)	-1.14 (25)	2.022 (2)	2.099 (2)
R = F, 1d ^d	7.3 (8)	-1.24 (7)	2.024 (2)	2.1038 (18)
R = Cl, 1e	10.3 (8)	-1.45 (5)	1.994 (11)	2.172 (9)
R = CN, 1f	9.1 (36)	-1.37 (30)	2.025 (3)	2.094 (2)
R = Me, 1g	1.5 (8)	-0.24 (34)	2.0208 (16)	2.0955 (13)
R = ⁱ Pr, 1h	1.7 (8)	-0.35 (28)	2.032 (6)	2.099 (5)
R = ^t Bu, 1i	1.8 (8)	-0.36 (28)	2.032 (3)	2.097 (2)

^aNumbers in parentheses are standard deviations. Bond distances observed in X-ray structures of metallacycles **2a-2i**. ^bX-ray data from ref. 5. ^cX-ray data from ref. 16. ^dX-ray data from ref. 18. ^ecrystal is an inversion twin - distances not reliable.

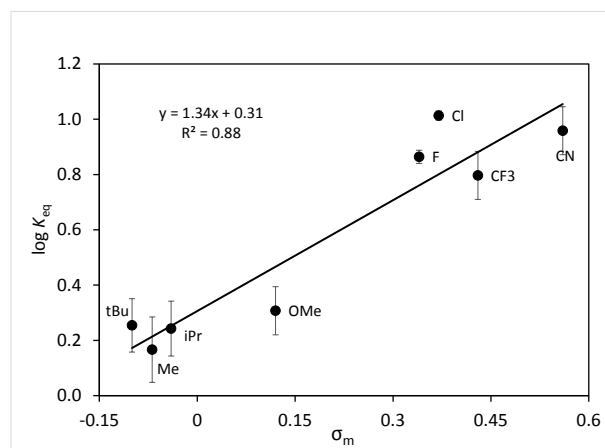


Figure 2. Hammett plot of $\log K_{eq}$ values for equilibria vs. σ_m .

Relative Rhodium-Carbon Bond Strengths. Homolytic bond strengths for the corresponding ortho-aryl C–H bond that undergoes activation were calculated at the B3LYP/6-311g* level of theory by comparing energies of the substituted phenylpyridines **1a-i** vs. the corresponding radicals **3a-i**. The relative rhodium-carbon homolytic bond strengths, D_{rel} , can be estimated by eq 2, where ΔG corresponds to the experimentally measured equilibrium constant for exchanging one substrate for unsubstituted 2-phenylpyridine as in eq 1, and $D(CH)_H$ and $D(CH)_R$ represent the homolytic C–H bond strengths of 2-phenylpyridine and the substituted 2-phenylpyridine respectively. ΔS for the equilibration is anticipated to be zero.

$$D_{rel} = \Delta G - [D(CH)_H - D(CH)_R] \quad (2)$$

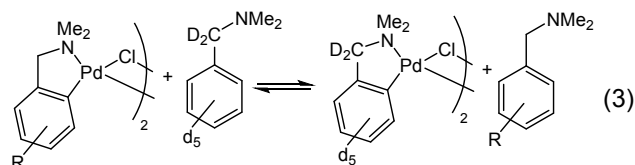
However, calculation of the ortho C–H homolytic bond strengths in **1a - 1i** at the B3LYP/6-311g* level of theory showed little variation at all (± 1 kcal/mol; see Supporting

Information, Fig. S28), and no trend was seen between homolytic Rh–C bond strengths and the homolytic D_{C-H} (see Fig. S32). The polar nature of these C–H activations suggested that the Rh–C bond strengths in the metallacycle products may correlate better to the *heterolytic* C–H bond strengths, which were also calculated B3LYP/6-311g* level of theory from the anions **4a-i** (see Supporting Information). A plot of the homolytic $D_{rel}(\text{Rh-C})$ vs. these heterolytic C–H bonds strengths showed only a modest correlation (see Fig. S31) with a slope of +0.11 ($R^2 = 0.88$).

The data are scattered, as the range of $D_{rel}(\text{Rh-C})$ spans only ~2 kcal/mol range, and is comparable to the errors in the K_{eq} measurements. The fact that the slope is far less than 1.0 indicates that one pays a higher price for breaking a strong C–H bond than one gains in the strength of the Rh–C bond that is formed. Therefore, substrates with larger heterolytic C–H bond strengths (i.e., less acidic) are less favorable to activate than substrates with weaker heterolytic C–H bond strengths. Since substrates with electron-withdrawing groups have weaker heterolytic bond strengths, cyclometallation of these substrates is preferred.

A recent report by Davies and Macgregor investigated similar substituent effects on the CMD activation of 1-phenylpyrazoles by $[\text{Cp}^*\text{MCl}_2]_2$ (M = Rh, Ir) in the presence of carboxylate.¹⁹ These studies showed that substrates with electron-donating substituents were *kinetically* favored, but that substrates with electron-withdrawing substituents were *thermodynamically* favored, as also seen here. A plot of $\log K_{eq}$ vs. $\sigma_{m,p}$ showed a slope of 1.46 with $R^2 = 0.90$, comparable to what is seen in Figure 2.

It is also worth comparing these results to those found earlier by Ryabov in his investigations of cyclometallation of N,N-dimethylbenzylamines by $\text{Pd}(\text{OAc})_2$.²⁰ In these studies, a dimeric acetate-bridged metallacycle underwent exchange with deuterated N,N-dimethylbenzylamine (eq 3), and acetic acid was necessary to carry out the protonation. Under these conditions, the protonolysis was the rate determining step for the exchange, and it was noted that Pd(II) will orthometallate preferably a ligand with a stronger electron-withdrawing group, as seen here.



CONCLUSIONS

Here we present evidence for the equilibration of para-substituted phenylpyridines in the concerted metallation-deprotonation reaction with pentamethylcyclopentadienylrhodium(III) in the presence of NaOAc/HOAc buffer. The results show that substrates with electron-withdrawing groups present in the para-position are preferred thermodynamically, as seen with palladium metallacycles.²⁰ This result is somewhat unexpected, as it might have been expected that the electrophilic CMD reactions would prefer substrates with electron-donating substituents. These results can be explained in that the heterolytic C–H bond strengths are weaker for the substrates with electron-withdrawing groups, and it is the breaking of this C–H bond that dominates the thermodynamics.

EXPERIMENTAL SECTION

General Information. RhCl₃ was obtained from Pressure Chemical Co. and [Cp*RhCl₂]₂ was synthesized using literature methods.²¹ 2-(4-trifluoromethylphenyl)pyridine, 2-(4-fluorophenyl)pyridine, 2-(4-chlorophenyl)pyridine, 4-(pyridine-2-yl)benzotrile, 2-(4-methylphenyl)pyridine, 2-(4-isopropylphenyl)pyridine, and 2-(4-tertbutylphenyl)pyridine were synthesized according to literature procedures.²² 2-phenylpyridine and 4-(2-pyridinyl)anisole were obtained from TCI America and used without further purification. Sodium acetate was obtained from JT Baker and used without further purification. Methanol was purchased from Fischer Chemical, dried over 3 Å molecular sieves, and filtered through PTFE syringe filters prior to use. Methanol-*d*₃ was obtained from Cambridge Isotope Labs Inc., dried over 3 Å molecular sieves, and transferred by vacuum distillation directly into J-Young NMR tubes for use. Chloroform-*d* was obtained from Cambridge Isotope Labs Inc., dried over 3 Å sieves, and filtered through a plug of Celite prior to use. All reactions were performed under N₂ atmosphere; however once the reactions were complete, further isolation of compounds was performed with no precaution to avoid atmosphere as the compounds are stable. All NMR spectra were collected using an Avance 400 NMR Spectrometer. Elemental analyses were determined at the CENTC Elemental Analysis Facility at the University of Rochester using a PerkinElmer 2400 Series II analyzer equipped with a PerkinElmer Model AD-6 autobalance by Dr. William W. Brennessel.

Synthesis. Preparation of 2a.⁵ A mixture of [Cp*RhCl₂]₂ (0.10 mmol, 61 mg, 0.50 equiv), 2-phenylpyridine (0.22 mmol, 34 mg, 1.1 equiv), and sodium acetate (0.40 mmol, 32 mg, 2.0 equiv) was stirred in (dry) methanol (25 mL), under a nitrogen atmosphere for 4 h. The solvent was evaporated to dryness on a rotovap. The crude material was purified via column chromatography (1:1 hex:EtOAc to 100% EtOAc) to give an orange-red solid (70.3 mg, 74.7%). ¹H NMR (400 MHz, CDCl₃) δ 8.73 (d, *J* = 5.4 Hz, 1 H), 7.81 (d, *J* = 7.8 Hz, 1 H), 7.75 (d, *J* = 7.8 Hz, 1 H), 7.69 (ddd, *J* = 8.2, 7.2, 1.6 Hz, 1 H), 7.60 (dd, *J* = 7.7, 1.4 Hz, 1 H), 7.24 (td, *J* = 7.4, 1.5 Hz, 1 H), 7.12 (ddd, *J* = 7.2, 5.6, 1.5 Hz, 1 H), 7.05 (td, *J* = 7.4, 1.1 Hz, 1 H), 1.62 (s, 15 H). ¹³C{¹H} NMR (101 MHz, CDCl₃) δ 178.6 (d, *J* = 32 Hz, Rh-C), 165.5, 151.4, 143.8, 137.1, 137.0, 130.5, 123.5, 122.8, 122.0, 119.1, 96.0 (d, *J* = 6.3 Hz, Rh-C), 9.3 (s, C₅Me₅).

Preparation of 2b.¹⁶ The reaction was carried out as with 2a, using [Cp*RhCl₂]₂ (0.10 mmol, 61 mg, 0.50 equiv), 4-(2-pyridinyl)anisole (0.22 mmol, 41 mg 1.1 equiv), and sodium acetate (0.40 mmol, 32 mg, 2.0 equiv) in methanol (25 mL). The product was purified via column chromatography (1:1 hex:EtOAc to 100% EtOAc) to give an orange-red solid (80.1 mg, 79.6%). ¹H NMR (400 MHz, CDCl₃) δ 8.66 (d, *J* = 5.6 Hz, 1 H), 7.69 – 7.58 (m, 2 H), 7.54 (d, *J* = 8.5 Hz, 1 H), 7.36 (d, *J* = 2.5 Hz, 1 H), 7.04 (td, *J* = 6.2, 2.3 Hz, 2 H), 6.61 (dd, *J* = 8.5, 2.5 Hz, 1 H), 3.90 (s, 3 H), 1.63 (s, 15 H). ¹³C{¹H} NMR (101 MHz, CDCl₃) δ 180.8 (d, *J* = 32 Hz, Rh-C), 165.3, 160.6, 151.2, 137.0, 137.0, 124.6, 121.3, 121.0, 118.5, 109.4, 96.0 (d, *J* = 6.3 Hz, Rh-C), 55.3, 9.3 (s, C₅Me₅). Anal. Calcd for C₂₂H₂₅NOCIRh; C, 57.20; H, 5.50; N, 3.06. Found: C, 57.38; H, 5.50; N, 2.84.

Preparation of 2c. The reaction was carried out as with 2a, using [Cp*RhCl₂]₂ (0.10 mmol, 61 mg, 0.5 equiv), 2-(4-trifluoromethylphenyl)pyridine (0.22 mmol, 49 mg 1.1 equiv), and sodium acetate (0.40 mmol, 32 mg, 2.0 equiv) in methanol

(25 mL). The product was purified via column chromatography (1:1 hex:EtOAc to 100% EtOAc) and was isolated as a red-orange solid (98.2 mg 90.0%). ¹H NMR (400 MHz, CDCl₃) δ 8.76 (d, *J* = 5.6 Hz, 1 H), 8.06 (s, 1 H), 7.82 (d, *J* = 8.0 Hz, 1 H), 7.75 (td, *J* = 7.8, 1.4 Hz, 1 H), 7.66 (d, *J* = 8.1 Hz, 1 H), 7.29 (d, *J* = 8.1 Hz, 1 H), 7.22 (td, *J* = 6.4, 5.6, 1.5 Hz, 1 H), 1.63 (s, 15 H). ¹³C{¹H} NMR (101 MHz, CDCl₃) δ 178.5 (d, *J* = 32.8 Hz, Rh-C), 168.8, 164.1, 151.6, 147.1, 137.6, 133.3, 133.3, 123.2, 123.1, 120.0, 96.4 (d, *J* = 6.1 Hz, Rh-C), 9.3. Anal. Calcd for C₂₂H₂₂NF₃ClRh; C, 53.30; H, 4.47; N, 2.83. Found: C, 53.29; H, 4.16; N, 2.30.

Preparation of 2d.¹⁸ The reaction was carried out as with 2a, using [Cp*RhCl₂]₂ (0.10 mmol, 61 mg, 0.5 equiv), 2-(4-fluorophenyl)pyridine (0.22 mmol, 38 mg 1.1 equiv), and sodium acetate (0.40 mmol, 32 mg, 2.0 equiv) in methanol (25 mL). The product was purified via column chromatography (1:1 hex:EtOAc to 100% EtOAc) and was isolated as a red-orange solid (81.0 mg, 82.6%). ¹H NMR (400 MHz, CDCl₃) δ 8.70 (d, *J* = 5.6 Hz, 1 H), 7.70 (dd, *J* = 6.6, 1.7 Hz, 2 H), 7.58 (dd, *J* = 8.5, 5.3 Hz, 1 H), 7.50 (dd, *J* = 8.8, 2.6 Hz, 1 H), 7.12 (td, *J* = 6.0, 2.4 Hz, 1 H), 6.75 (td, *J* = 8.7, 2.6 Hz, 1 H), 1.62 (s, 15 H). ¹³C{¹H} NMR (101 MHz, CDCl₃) δ 181.4 (d, *J* = 29.1 Hz, Rh-C), 164.5, 162.1, 151.3, 140.0, 137.3, 124.7 (d, *J* = 8.7 Hz, F-C), 122.8 (d, *J* = 101.2 Hz, F-C), 121.9, 119.1, 110.1 (d, *J* = 96.3 Hz, F-C), 96.2 (d, *J* = 6.2 Hz, Rh-C), 9.2.

Preparation of 2e. The reaction was carried out as with 2a, using [Cp*RhCl₂]₂ (0.10 mmol, 61 mg, 0.5 equiv), 2-(4-chlorophenyl)pyridine (0.22 mmol, 41 mg 1.1 equiv), and sodium acetate (0.40 mmol, 32 mg, 2.0 equiv) in methanol (25 mL). The product was purified via column chromatography (1:1 hex:EtOAc to 100% EtOAc) and was isolated as a red-orange solid (85.0 mg, 83.6%). ¹H NMR (400 MHz, CDCl₃) δ 8.70 (d, *J* = 5.6 Hz, 1 H), 7.75 (d, *J* = 2.0 Hz, 1 H), 7.70 (d, *J* = 4.1 Hz, 2 H), 7.50 (d, *J* = 8.1 Hz, 1 H), 7.17 – 7.11 (m, 1 H), 7.02 (dd, *J* = 8.2, 2.0 Hz, 1 H), 1.62 (s, 15 H). ¹³C{¹H} NMR (101 MHz, CDCl₃) δ 180.0 (d, *J* = 33.3 Hz Rh-C), 164.5, 151.4, 142.3, 137.4, 136.2, 135.8, 124.3, 123.2, 122.4, 119.3, 96.2 (d, *J* = 6.0 Hz, Rh-C), 9.3 (C₅Me₅). Anal. Calcd for C₂₁H₂₂NCl₂Rh; C, 54.57; H, 4.80; N, 3.03. Found: C, 52.94; H, 4.51; N, 2.94.

Preparation of 2f. The reaction was carried out as with 2a, using [Cp*RhCl₂]₂ (0.10 mmol, 61 mg, 0.5 equiv), 4-(pyridine-2-yl)benzotrile (0.22 mmol, 40 mg 1.1 equiv), and sodium acetate (0.40 mmol, 32 mg, 2.0 equiv) in methanol (25 mL). The product was purified as an orange-red solid via column chromatography (1:1 hex:EtOAc to 100% EtOAc) and was isolated as a red orange solid (69.6 mg, 69.9%). ¹H NMR (400 MHz, CDCl₃) δ 8.71 (d, *J* = 5.6 Hz, 1 H), 7.92 – 7.63 (m, 3 H), 7.52 (d, *J* = 8.2 Hz, 1 H), 7.15 (q, *J* = 4.9 Hz, 1 H), 7.03 (d, *J* = 8.1 Hz, 1 H), 1.62 (s, 15 H). ¹³C{¹H} NMR (101 MHz, CDCl₃) δ 178.3 (d, *J* = 34.3 Hz), 163.6, 151.7, 148.0, 140.0, 137.7, 126.6, 123.7, 123.1, 120.4, 120.1, 112.9, 96.5 (d, *J* = 7.0 Hz Rh-C), 9.3 (C₅Me₅). Anal. Calcd for C₂₂H₂₂N₂ClRh; C, 58.36; H, 4.99; N, 6.19. Found: C, 58.04; H, 4.71 N, 6.06.

Preparation of 2g. The reaction was carried out as with 2a, using [Cp*RhCl₂]₂ (0.10 mmol, 61 mg, 0.5 equiv), 2-(4-methylphenyl)pyridine (0.22 mmol, 37 mg 1.1 equiv), and sodium acetate (0.40 mmol, 32 mg, 2.0 equiv) in methanol (25 mL). The product was purified via column chromatography (1:1 hex:EtOAc to 100% EtOAc) and was isolated as an orange-red solid (78.1 mg, 80.4%). ¹H NMR (400 MHz, CDCl₃) δ 8.70 (d, *J* = 5.5 Hz, 1 H), 7.81 – 7.57 (m, 2 H), 7.48 (d, *J* = 7.8 Hz, 1 H), 7.07 (t, *J* = 6.3 Hz, 1 H), 6.86 (d, *J* = 7.7 Hz, 1 H), 2.40 (s, 3 H), 1.62 (s, 15 H). ¹³C{¹H} NMR (101 MHz, CDCl₃) δ 178.7 (d, *J*

= 32 Hz, Rh-C), 165.6, 151.3, 141.2, 140.3, 137.6, 137.0, 124.0, 123.3, 121.5, 118.8, 95.9 (d, $J = 6.0$ Hz, Rh-C), 21.9, 9.3 (C₅Me₅). Anal. Calcd for C₂₂H₂₅NCIRh: C, 59.81; H, 5.70; N, 3.17. Found: C, 59.96; H, 5.62; N, 2.96.

Preparation of 2h. The reaction was carried out as with **2a**, using [Cp*RhCl₂]₂ (0.10 mmol, 61 mg, 0.5 equiv), 2-(4-isopropylphenyl)pyridine (0.22 mmol, 43 mg 1.1 equiv), and sodium acetate (0.40 mmol, 32 mg, 2.0 equiv) in methanol (25 mL). The product was purified via column chromatography (1:1 hex:EtOAc to 100% EtOAc) and was isolated as an orange-red solid (72.5 mg, 70.1%). ¹H NMR (400 MHz, CDCl₃) δ 8.67 (d, $J = 5.5$ Hz, 1 H), 7.72–7.59 (m, 2 H), 7.50 (d, $J = 7.9$ Hz, 1 H), 7.05 (ddd, $J = 7.2, 5.6, 1.7$ Hz, 1 H), 6.90 (dd, $J = 7.9, 1.7$ Hz, 1 H), 2.95 (hept, $J = 6.9$ Hz, 1 H), 1.60 (s, 15 H), 1.30 (dd, $J = 6.9, 2.9$ Hz, 6 H). ¹³C{¹H} NMR (101 MHz, CDCl₃) δ 178.7 (d, $J = 32.3$ Hz Rh-C), 165.5, 151.3, 150.9, 141.6, 137.0, 135.2, 123.4, 121.5, 121.2, 118.8, 96.0, 95.9 (d, $J = 7.0$ Hz Rh-C), 34.6, 24.7, 23.7, 9.3 (C₅Me₅). Anal. Calcd for C₂₄H₂₉NCIRh: C, 61.35; H, 6.22; N, 2.98. Found: C, 59.35; H, 6.37; N, 3.35.

Preparation of 2i. The reaction was carried out as with **2a**, using [Cp*RhCl₂]₂ (0.10 mmol, 61 mg, 0.5 equiv), 2-(4-tertbutylphenyl)pyridine (0.22 mmol, 46 mg 1.1 equiv), and sodium acetate (0.40 mmol, 32 mg, 2.0 equiv) in methanol (25 mL). The product was purified via column chromatography (1:1 hex:EtOAc to 100% EtOAc) and was isolated as an orange-red solid (75.5 mg 70.6%). ¹H NMR (400 MHz, CDCl₃) δ 8.70 (d, $J = 5.4$ Hz, 1 H), 7.86 (d, $J = 1.7$ Hz, 1 H), 7.68 (ddd, $J = 13.7, 8.6, 6.9$ Hz, 2 H), 7.58–7.48 (m, 1 H), 7.09 (tdd, $J = 7.1, 4.3, 2.7$ Hz, 2 H), 1.62 (s, 15 H), 1.40 (s, 9 H). ¹³C{¹H} NMR (101 MHz, CDCl₃) δ 178.5 (d, $J = 31.8$ Hz, Rh-C), 165.5, 152.8, 151.3, 141.2, 137.0, 133.7, 123.1, 121.5, 120.4, 118.8, 97.0 (d, $J = 6.4$ Hz, Rh-C), 35.3, 31.6, 9.3 (C₅Me₅). Anal. Calcd for C₂₅H₃₁NCIRh: C, 62.05; H, 6.55; N, 2.90. Found: C, 61.54; H, 6.38; N, 2.93.

Example Equilibration Experiment. C–H activated complexes for equilibration experiments were generated in situ from stock solutions to improve reproducibility. 1 mL of a 5 mM (0.5 equiv, 0.005 mmol) solution of [Cp*RhCl₂]₂ in methanol, 0.5 mL of a 20 mM (1 equiv, 0.01 mmol) solution of 2-phenylpyridine in methanol, and 0.5 mL of a 100 mM (5 equiv, 0.05 mmol) solution of sodium acetate in methanol, were charged into a J-Young type NMR tube. Protonated methanol was removed in vacuo, and approximately 0.5 mL of deuterated methanol was transferred into the NMR tube on a vacuum line. Once complete disappearance of the unactivated 2-phenylpyridine was observed via ¹H NMR spectroscopy, the NMR tube was opened under a blanket of nitrogen, and 0.5 mL of a 20 mM (1 equiv, 0.01 mmol) solution of 4-(2-pyridinyl)anisole was charged into the NMR tube. The NMR tube was resealed, the reaction was evaporated to dryness, and fresh deuterated methanol was transferred in on a vacuum line. The NMR tube was reopened under a blanket of nitrogen, and 2.85 μL (5 equiv, 0.05 mmol) of glacial acetic acid was charged into the solution. After three cycles of freeze-pump-thaw-degassing, the NMR tube was backfilled with 1 atm of N₂ and heated to 40 °C. This procedure was followed with another NMR tube, but this time, generating the 4-(2-pyridinyl)anisole C–H activated complex first, and charging with 2-phenylpyridine second. Both reactions were monitored via ¹H NMR spectroscopy daily, until Q_{eq} calculated via the relative integrations of the iminyl proton of each reaction were the same. Convergence to the same Q_{eq} value indicated that the reaction had reached equilibrium.

Computational Information. Geometry optimizations and frequency calculations were performed on phenylpyridines **1a-i**, radicals **3a-i**, and anions **4a-i** using the Gaussian 09 software package, at the B3LYP/6-311g* level of theory. Homolytic and heterolytic C–H bond dissociation energies were calculated with from these enthalpies.

ASSOCIATED CONTENT

Supporting Information

The Supporting Information is available free of charge on the ACS Publications website at DOI: 10.1021/acs.joc.xxxxxxxx.

Detailed information regarding NMR spectra, X-ray data, computational analysis, (PDF)

X-ray data for compound **2c** (CIF)

X-ray data for compound **2e** (CIF)

X-ray data for compound **2f** (CIF)

X-ray data for compound **2g** (CIF)

X-ray data for compound **2h** (CIF)

X-ray data for compound **2i** (CIF)

Full structural details are available from the Cambridge Crystallographic Data Centre (CCDC #1936428-1936433).

AUTHOR INFORMATION

Corresponding Author

*E-mail: jones@chem.rochester.edu

ORCID

William D. Jones: 0000-0003-1932-0963

Andrew VanderWeide: 0000-0001-9486-3170

William W. Brennessel: 0000-0001-5461-1825

Notes

The authors declare no competing financial interest.

ACKNOWLEDGMENT

We thank the National Science Foundation, Chemistry-Physical Sciences: F.02 (award #CHE-1762350) for support for this work.

REFERENCES

- (1) *C–H Bond Activation and Catalytic Functionalization I and II*; Dixneuf, P. H.; Doucet, H., Eds.; Topics in Organometallic Chemistry; Springer International Publishing, 2016.
- (2) Thompson, J. M.; Heck, R. F. Carbonylation Reactions of Ortho-Palladation Products of α -Arylnitrogen Derivatives. *J. Org. Chem.* **1975**, *40*, 2667–2674.
- (3) Pfeffer, M. Selected Applications to Organic Synthesis of Intramolecular C–H Activation Reactions by Transition Metals. *Pure Appl. Chem.* **1992**, *64*, 335–342.
- (4) Abbenhuis, H. C. L.; Pfeffer, M.; Sutter, J. P.; de Cian, A.; Fischer, J.; Ji, H. L.; Nelson, J. H. Carbon–Carbon and Carbon–Nitrogen Bond Formation Mediated by Ruthenium(II) Complexes: Synthesis of (1H)-Isoquinolinium Derivatives. *Organometallics* **1993**, *12*, 4464–4472.
- (5) Li, L.; Brennessel, W. W.; Jones, W. D. An Efficient Low-Temperature Route to Polycyclic Isoquinoline Salt Synthesis via C–H Activation with [Cp*MCl₂]₂ (M = Rh, Ir). *J. Am. Chem. Soc.* **2008**, *130*, 12414–12419.
- (6) Stuart, D. R.; Bertrand-Laperle, M.; Burgess, K. M. N.; Fagnou, K. Indole Synthesis via Rhodium Catalyzed Oxidative Coupling of Acetanilides and Internal Alkynes. *J. Am. Chem. Soc.* **2008**, *130*, 16474–16475.
- (7) Guimond, N.; Fagnou, K. Isoquinoline Synthesis via Rhodium-Catalyzed Oxidative Cross-Coupling/Cyclization of Aryl Aldimines and Alkynes. *J. Am. Chem. Soc.* **2009**, *131*, 12050–12051.

(8) Ryabov, A. D.; Sakodinskaya, I. K.; Yatsimirsky, A. K. Kinetics and Mechanism of Ortho-Palladation of Ring-Substituted N,N-Dimethylbenzylamines. *J. Chem. Soc., Dalton Trans.* **1985**, 2629–2638.

(9) Ritleng, V.; Sirlin, C.; Pfeffer, M. Ru-, Rh-, and Pd-Catalyzed C–C Bond Formation Involving C–H Activation and Addition on Unsaturated Substrates: Reactions and Mechanistic Aspects. *Chem. Rev.* **2002**, *102*, 1731–1770.

(10) Davies, D. L.; Al-Duaij, O.; Fawcett, J.; Giardiello, M.; Hilton, S. T.; Russell, D. R. Room-Temperature Cyclometallation of Amines, Imines and Oxazolines with $[MCl_2Cp^*]_2$ (M = Rh, Ir) and $[RuCl_2(p\text{-Cymene})]_2$. *Dalton Trans.* **2003**, 4132–4138.

(11) Davies, D. L.; Donald, S. M. A.; Macgregor, S. A. Computational Study of the Mechanism of Cyclometallation by Palladium Acetate. *J. Am. Chem. Soc.* **2005**, *127*, 13754–13755.

(12) Davies, D. L.; Donald, S. M. A.; Al-Duaij, O.; Macgregor, S. A.; Pölleth, M. Electrophilic C–H Activation at $\{Cp^*Ir\}$: Ancillary-Ligand Control of the Mechanism of C–H Activation. *J. Am. Chem. Soc.* **2006**, *128*, 4210–4211.

(13) Davies, D. L.; Donald, S. M. A.; Al-Duaij, O.; Fawcett, J.; Little, C.; Macgregor, S. A. N–H versus C–H Activation of a Pyrrole Imine at $\{Cp^*Ir\}$: A Computational and Experimental Study. *Organometallics* **2006**, *25*, 5976–5978.

(14) Lapointe, D.; Fagnou, K. Overview of the Mechanistic Work on the Concerted Metallation–Deprotonation Pathway. *Chem. Lett.* **2010**, *39*, 1118–1126.

(15) Li, L.; Brennessel, W. W.; Jones, W. D. C–H Activation of Phenyl Imines and 2-Phenylpyridines with $[Cp^*MCl_2]_2$ (M = Ir, Rh): Regioselectivity, Kinetics, and Mechanism. *Organometallics* **2009**, *28*, 3492–3500.

(16) Walsh, A. P.; Jones, W. D. Mechanistic Insights of a Concerted Metalation-Deprotonation Reaction with $[Cp^*RhCl_2]_2$. *Organometallics* **2015**, *34*, 3400–3407.

(17) For X-ray structure of **2a** see ref. 5. For X-ray structure of **2b** see ref. 16. For X-ray structure of **2d** see ref. 18.

(18) Brasse, M.; Cámpora, J.; Ellman, J. A.; Bergman, R. G. Mechanistic Study of the Oxidative Coupling of Styrene with 2-Phenylpyridine Derivatives Catalyzed by Cationic Rhodium(III) via C–H Activation. *J. Am. Chem. Soc.* **2013**, *135*, 6427–6430.

(19) Alharis, R. A.; McMullin, C. L.; Davies, D. L.; Singh, K.; Macgregor, S. A. The Importance of Kinetic and Thermodynamic Control When Assessing Mechanisms of Carboxylate-Assisted C–H Activation. *J. Am. Chem. Soc.* **2019**, *141*, 8896–8906.

(20) Ryabov, A. D. Thermodynamics, Kinetics, and Mechanism of Exchange of Cyclopalladated Ligands. *Inorg. Chem.* **1987**, *26*, 1252–1260.

(21) Kang, J. W.; Moseley, K.; Maitlis, P. M., Pentamethylcyclopentadienylrhodium and -Iridium Halides. I. Synthesis and Properties. *J. Am. Chem. Soc.* **1969**, *91*, 5970–5977.

(22) Zou, Y. J.; Yue, G. Z.; Xu, J. W.; Zhou, J. R., General Suzuki Coupling of Heteroaryl Bromides by Using Tri-tert-butylphosphine as a Supporting Ligand. *Eur. J. Org. Chem.* **2014**, *27*, 5901–5905.